Research Article

Nano Biomed Eng

DFT-Quantum Chemical and Experimental Studies of a New 2-(Substituted Thio) Furan as a Corrosion Inhibitor in Acidic Media

Israa M. H. Al-mousawi✉, Noor Ali Khudhair, Lama S. Ahmed
Department of Chemistry, College of Science, University of Baghdad.

✉ Corresponding authors. E-mail: israamousawi@gmail.com

Received: Nov. 5, 2021; **Accepted:** Sep. 19, 2022; **Published:** Oct. 20, 2022

Citation: Israa M. H. Al-Mousawi, Noor Ali Khudhair, and Lama S. Ahmed,DFT-Quantum Chemical and Experimental Studies of a New 2-(Substituted Thio) Furan as a Corrosion Inhibitor in Acidic Media. *Nano Biomed. Eng.*, 2022, 14(2): 136-148.
DOI: 10.5101/nbe.v14i2.p136-148.

Abstract

The corrosion inhibiting properties of the new furan derivative 5-(furan-2-ylmethylsulfonyl-4-phenyl-2,4-dihydro [1,2,4] triazole-3-thione in acidic solution (1.0 M HCl) were explored utilizing electrochemical, surface morphology (AFM), and quantum chemical calculations approaches. The novel furan derivative 5-(furan-2-ylmethylsulfonyl-4-phenyl-2,4-dihydro [1,2,4] triazole-3-thione shows with an inhibitory efficiency value of 99.4 percent at 150 ppm, carbon steel corrosion in acidic medium is effectively inhibited, according to the results. The influence of temperature on corrosion prevention was studied using adsorption parameters and activation thermodynamics. The novel furan derivative creates a protective layer over the metallic surface that separates the metal from harsh acid solution and thereby protects it from destructive disintegration, according to the AFM study. The experimental findings are supported by the theoretical method of density functional theory (DFT) at the B3LYP/6-311 ++G basis set for inhibitor.

Keywords: DFT, Corrosion inhibitors, Tafel polarization, Furan

Introduction

Corrosion is a chemical or electrochemical interaction that occurs between materials, usually a metal, and their environment, resulting in the materials' and their qualities deteriorating. Corrosion inhibitors are commonly used to decrease the amount of unwanted base metal dissolving caused by these processes. To preserve metallic components from corrosion, the hunt for new and effective corrosion inhibitors, particularly in hydrochloric acid solutions, has become a necessity [1-3]. Adsorption of organic inhibitor molecules (physically or chemically) is widespread across the metal surface, and the resulting adsorption layer serves as a corrosion barrier. This shows that the most important characteristics in selecting an inhibitor molecule are hydrophobicity, molecular structure, and electron density at donor-atoms, solubility, and dispersibility [4-6]. The majority of organic inhibitor compounds contain heteroatoms such as N, O, S and numerous Pi bonds in their molecules facilitate adsorption on the steel surface [7-8].

Thiocarbanilide was prevented electrochemical corrosion of high carbon steel in 1 M sulfuric acid and hydrochloric acid solutions, the thiocarbanilide efficiently inhibited carbon steel at all concentrations, with an average inhibition efficiency of roughly 70%

in sulfuric acid and 80% in hydrochloric acid [9]. In addition, phenyltetrazole compounds were shown to be effective inhibitors of mild steel corrosion in a 5.0 M HCl solution, acting as cathodic type inhibitors [10]. While Tetrahydropyridine derivatives are excellent mild steel inhibitors in 1 M hydrochloric acid [11].

As well as the experimental studies, quantum chemical calculations are used to examine the correlation between electronic structure and corrosion inhibition capability [12]. Further, a theoretical study grants the pre-selection of compounds with the fundamental structural essence to act as organic corrosion inhibitors.

The purpose of this research is to look at the corrosion inhibitory properties of the new furan derivative 5-(furan-2-ylmethylsulfonyl-4-phenyl-2,4-dihydro [1,2,4] triazole-3-thione (FMSPhDHT) for carbon steel corrosion prevention in acidic solution (1 M HCl). Luma S. A. synthesized and characterized the FMSPhDHT ($C_{14}H_{13}N_3OS_2$) as shown in Fig. 1 [13]. To establish the molecule's electronic structure, we used the electrochemical (anodic and cathodic Tafel polarization) method and quantum chemical calculations utilizing the density function theory (DFT).

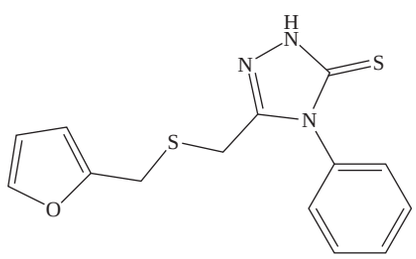

Fig. 1 Structure of 5-(furan-2-ylmethylsulfonyl-4-phenyl-2,4-dihydro [1,2,4] triazole-3-thione.

Experimental

Chemicals

The chemical materials were used in this work are shown in Table 1.

Preparation of carbon steel samples

Table 2 shows the metallic components in carbon steel reinforcing bar (CSRB) as a proportion of the overall composition.

In order to learn more about the impacts of corrosion carbon steel was studied using samples in a circle with a diameter of 1.5 cm carbon steel samples were cleaned using one of the most well-known tools for preparation: immersion in hydrochloric acid to remove any oxide layer or impurities present on the metal's surface, followed by washing with distilled water. The samples were smoothed with silicon carbide smoothing papers ranging (80-2000). After that, the samples were washed thoroughly with distilled water until they were as glossy as a mirror and stored in a separate container.

Table 1 The chemical materials used in this study

No.	Materials	Molecular formula	Suppliers
1	Hydrochloric acid	HCl	BDH
2	dimethyl sulfoxide (DMSO)	$(CH_3)_2SO$	BDH
3	FMSPhDHT	$C_{14}H_{13}N_3OS_2$	locally created

Preparation of acid solution

In a volumetric flask with a volume of 1000 mL, the acid solution was made at a concentration of one molar, and the volume was completed to the mark with distilled water.

Corrosion Inhibitor FMSPHDHT Solution

FMSPHDHT powder was dissolved in dimethyl sulfoxide (DMSO) solvent and poured into a 10 mL volumetric flask to make three different concentrations (50, 100, and 150 ppm).

Corrosion Potential Measurements

The effect of the prepared compound FMSPHDHT in an acidic environment with one molar concentration was investigated using the electrical method (static stress polarization method) with circular carbon steel samples and a device (Advanced potentiostant winking MLab-200 (2007) [Bank Elektronik-Intelligent control GmbH]) as shown in Fig. 2, with three electrodes of corrosion cell and accompanying accessories were used. The corrosion cell is shown in Fig. 3, and the three electrodes were the first electrodes used as a reference, which was AgCl, Ag, and KCl (Ag/AgCl, 3.0 M KCl)) based on their potential. The second electrode is an auxiliary electrode made up of a platinum with a high purity rod, and the third is a working electrode (CS) with a 1.5 cm diameter that was installed on the

Table 2 Chemical composition of carbon steel reinforcing bar (CSRB) which are used in this study

Element	C%	S%	Si%	N%	Cu%	Mn%	Ni%	Cr%	p%
percentage	0.26	0.031	0.28	0.010	0.28	0.73	0.13	0.12	0.018

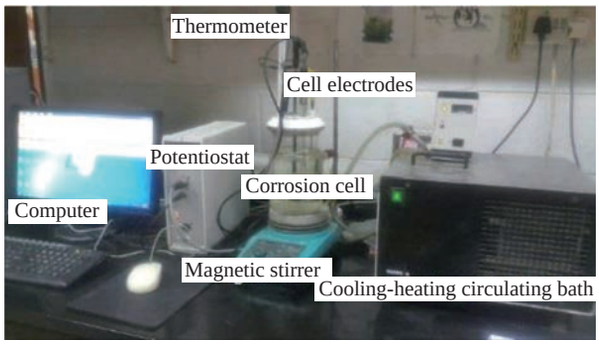

Fig. 2 Electrochemical system.

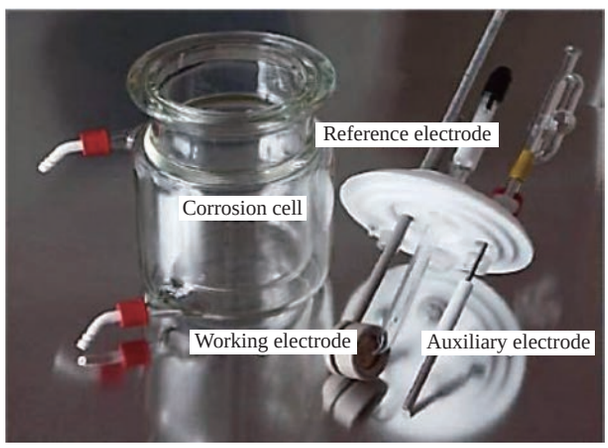

Fig. 3 Corrosion cell.

working electrode load and the acidic solution was exposed via the hole. The steps of measurement are:

- The corrosion cell was filled with just blank solution (1000 mL).

- The working electrode was carbon steel, the reference electrode was in front of it, and the auxiliary electrode was beside it.

- After around 15 minutes, the response starts for the first time. The initial run was accompanied with a Tafel plot. The temperature was then increased to 50 degrees Celsius.

- The inhibitor was then added to the blank solution at 25 degrees Celsius to get the first run, Tafel plot, and corrosion rate, as well as the data reported in Table 3.

- The temperature is raised to 30, 40, and 50 degrees Celsius, respectively, and the process is repeated for all inhibitor doses.

Results and Discussion

Potentiodynamic polarization measurement

Polarization curves were extracted for the corrosion of carbon steel in the acidic solution of the new prepared inhibitor FMSPHDHT at concentrations (50, 100, 150) parts per million (ppm) and at four different temperatures (298-323) Kelvin in the absence and presence of the inhibitor FMSPHDHT as shown in the Fig. 4.

Table 3 shows the electrochemical characteristics for carbon steel acid corrosion in the presence of different

Table 3 Polarization parameters for carbon steel in the absence and presence of various concentrations of FMSPHDHT in acidic solution

Comp. ppm	Temp.	E_{corr} (mV)	I_{corr} ($\mu A/cm^2$)	Bc (mV/Dec)	Ba (mV/Dec)	PL (mm/y)	IE%
blank	293	-239.7	157.54	-141.2	109.3	1.83	-
	303	-245.1	168.95	-160.8	135.0	1.96	-
	313	-276.9	176.10	-151.9	205.2	2.04	-
	323	-261.9	186.65	-131.2	219.9	2.17	-
50	293	-415.0	5.64	-321.0	442.5	0.0654	96.5
	303	-448.2	7.16	-397.5	605.3	0.0831	95.8
	313	-441.4	8.09	-483.5	511.1	0.0939	95.5
	323	-434.3	9.48	-423.6	470.2	0.110	95.0
100	293	-428.4	3.04	-228.4	216.0	0.0353	98.1
	303	-434.3	3.60	-249.6	242.1	0.0418	97.9
	313	-440.7	5.49	-393.5	446.7	0.0637	96.9
	323	-435.8	6.55	-413.1	422.4	0.0760	96.5
150	293	-440.6	0.98	-146.7	227.5	0.0114	99.4
	303	-441.8	1.10	-103.7	105.6	0.0128	99.4
	313	-440.2	1.99	-145.1	135.6	0.0231	98.9
	323	-429.0	3.82	-275.4	271.7	0.0443	98.0

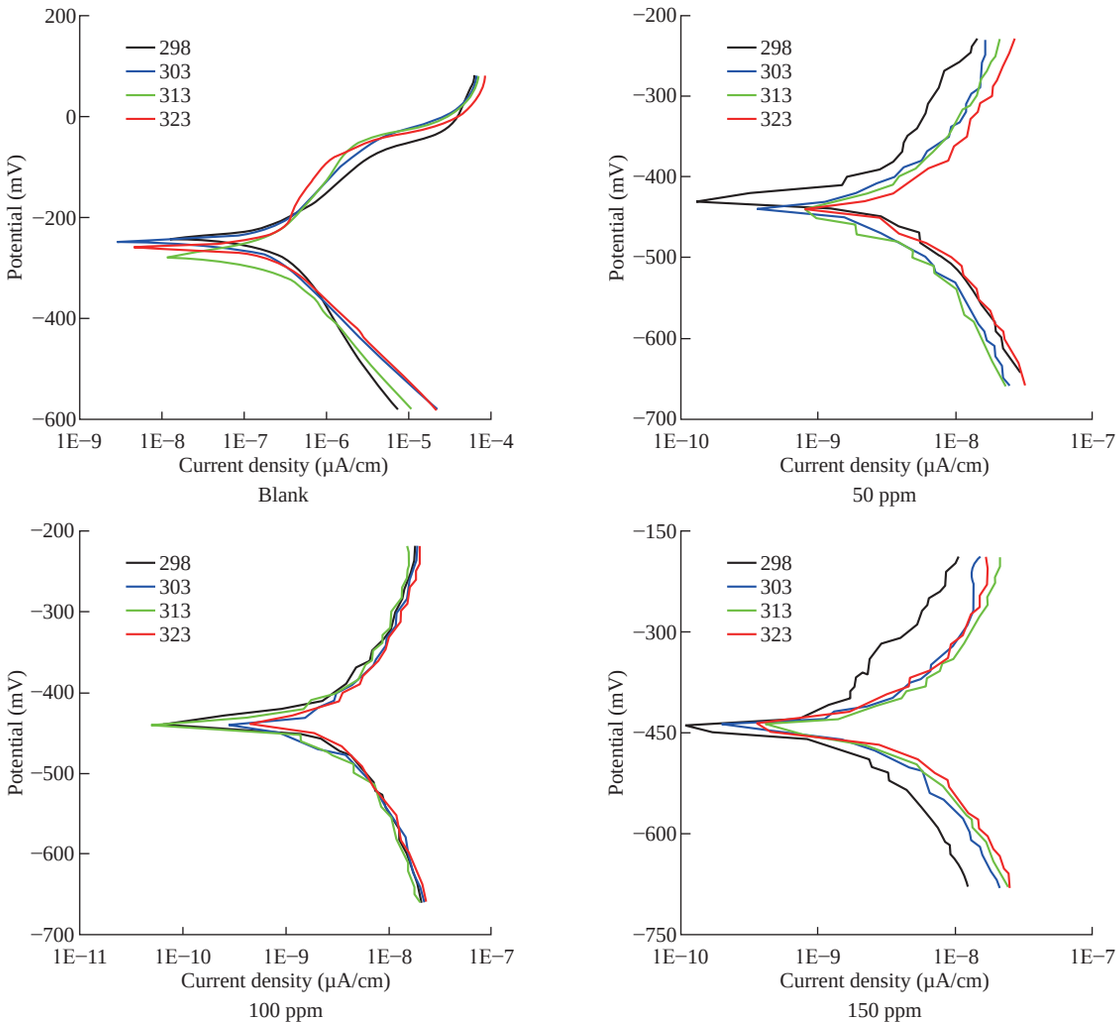

Fig. 4 Potentioatatic Polarization curves for carbon steel with absence and present of FMSPHDHT compound in 1 M HCl at different concentration.

concentrations of FMSPHDHT, such as corrosion potential (E_{corr}), corrosion current density (I_{corr}), Tafel slopes (bc and ba), and inhibition efficiencies (IE).

These findings reveal that the FMSPHDHT reduces the I_{corr} value at all concentrations, implying that this molecule is a good corrosion inhibitor. Furthermore, FMSPHDHT results in a minor change of E_{corr} to negative values and by raising inhibitor concentration, inhibition efficiency (percentage) improves. As a result, at a concentration of 150 ppm, FMSPHDHT had the highest inhibitory efficiency (99.4%) at 298 k, due to the presence of a high electronic density represented by the phenyl ring, as well as sulfur, three nitrogen atoms and Pi bonds, contribute to the formation of coordination bonds with the metal surface, resulting in the formation of a preservative layer for the metal in the acidic solution, which inhibits carbon steel [14-15]. The corrosion inhibition efficiency (IE) was estimated using the following formula from the corrosion current density.

$$IE\% = [I_{corr}\ (uncoated) - I_{corr}\ (coated)]/I_{corr}\ (uncoated) \times 100$$

where I_{corr} (uncoated) and I_{corr} (coated) are the corrosion current density values without and with inhibitor, respectively. The decreasing inhibition performance as the temperature of the solution rises might be explained to an increase in the mobility of the inhibitor molecules, resulting in a reduction in the contact between the inhibitor molecules and the carbon steel surface [16-17].

Kinetic and Thermodynamic of Corrosion

The influence of temperature on the efficacy of corrosion inhibition using the inhibitor FMSPHDHT at temperatures ranging from 293-323 K with and without the inhibitor is part of the thermodynamic investigation. The values of thermodynamic functions are shown in Table 4. After adding the inhibitor to

Table 4 Activation parameters of carbon steel corrosion in the absence and presence of inhibitor FMSPHDHT in 1 M HCl

Sample	T(K)	E_a (kJ/mole)	ΔH^* (kJ/mol)	ΔS^* (kJ/mol.K)	ΔG^* (kJ/mol)
Blank	293	4.333	1.776	-0.197	0.060
	303				0.062
	313				0.064
	323				0.066
50 ppm	293	13.255	10.698	-0.194	0.068
	303				0.07
	313				0.072
	323				0.074
100 ppm	293	21.424	18.867	-0.171	0.069
	303				0.071
	313				0.073
	323				0.075
150 ppm	293	36.485	33.929	-0.131	0.073
	303				0.074
	313				0.075
	323				0.077

the medium, the data reveal a noticeable difference. The addition of the inhibitor caused the reaction to be directed to locations with high activation energy values, slowing the corrosion rate. Arrhenius equation was used to compute the energy of the activation process [18]:

$$\text{Log } (i_{corr}) = \text{Log } A - E_a/2.303RT.$$

where A is the pre-exponential factor of Arrhenius, T is the absolute temperature, R is the gas constant and E_a the apparent activation energy of the corrosion reaction. The slope of the linear plot of log (i_{corr}) versus 1/T as shown in Fig. 5, as well as the activation energy values obtained mentioned in Table 4, were used to calculate E_a.

The activation parameters, activation enthalpy (ΔH^*), and activation entropy (ΔS^*), were computed using the Eyring transition state equation [19]:

$$\text{Log } (CR/T) = \text{Log } (R/Nh) + \Delta S^*/2.303R - \Delta H^*/2.303RT$$

CR stands for corrosion rate, h for Planck's constant, and N for Avogadro's number. Figure 6 transition stage was a plot of log(CR/T) vs 1/T produced a straight line with an intercept of [log(R/Nh) + (ΔS^*/2.303R)] and a slope of (ΔH^*/2.303R). ΔH^* and ΔS^* were calculated from this data and are listed in Table 4. The following thermodynamic relationship can be used to compute the change in activation free energy ΔG^* for the corrosion process at each temperature.

$$\Delta G^* = \Delta H^* - T\,\Delta S^*$$

Table 3 demonstrates that the value of H^* for carbon steel corrosion in acidic solution (1.776) in the absence of the inhibitor rose in the presence of the inhibitor, with the greatest value of the enthalpy of inhibition (150 ppm) indicating improved protection efficiency and an endothermic nature of the carbon steel dissolution [20]. The negative inhibitory entropy ΔS^* suggests a high degree of adsorption regularity during the activation phase, indicating the creation of the activated complex and a reduction in degrees of freedom [21-23]. The obtained values of ΔG^* are listed in Table 2. ΔG^* values were positive and increased slightly as temperature increased, indicating that the inhibitor lowered the thermodynamic feasibility of corrosion [24].

Surface study

Atomic force microscopy (AFM) was used to analyze the surface of a carbon steel sample in acid solution (1 M HCl) in the absence and presence of the inhibitor FMSPHDHT. Figure 5 shows that in the presence of the acidic solution, the surface topography of the steel sample has been damaged, and the surface roughness (40.7 nm) is clearly visible as shown in Fig. 7(a), but after adding the inhibitor FMSPHDHT, the surface roughness (7.78 nm) of the carbon steel has been reduced as clearly shown in Fig. 7(b) [25-26].

According to the results, the adsorption of these molecules at the metal-solution interface may explain the inhibitory effect of the novel furan derivative on carbon steel corrosion in 1 M HCl solution. The inhibitory effect of FMSPHDHT is related to the interaction of p-electrons phenyl and furan ring, as well as the presence of electron donor groups (N, O, and S) via which it forms bonds with carbon steel [27]

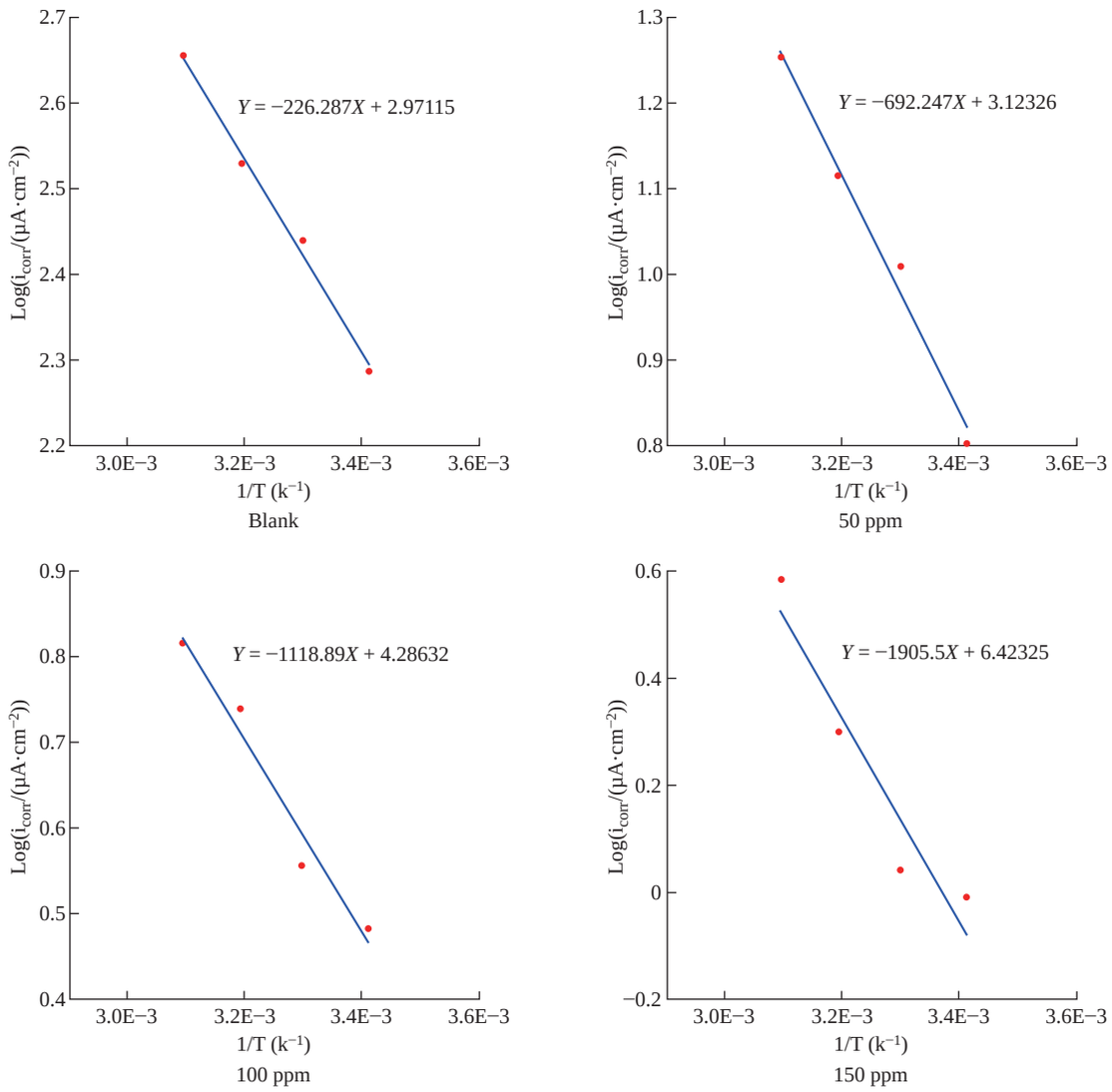

Fig. 5 Arrhenius plots for CS in 1 M HCl solution without and with varied quantities of additives inhibitor FMSPHDHT at different temperatures.

Computational study

Theoretical details

The structural and electronic properties of the new furan derivative 5-(furan-2-ylmethylsulfonyl-4-phenyl-2,4-dihydro [1,2,4] triazole-3-thione molecule were investigated using density functional theory (DFT) and frequency calculations at the Lee, Yang, and Parr (B3LYP/6-311++ G(d, p)) basis set [28]. All calculations were done with the Gaussian 09W program [29]. The structure of the molecule FMSPhDHT (Fig. 8) was drawn using the ChemDraw of Mopac tool (ver. 10), the bond lengths and dihedral angles are listed in Tables 5 and 6.

Molecular reactivity

The following relationships [30-31] are used to calculate quantum chemical parameters such as dipole moment (μ), electro negativity (χ), hardness (η), softness (S), ionization potential (IP), electron affinity (EA), the fractions of electrons transferred (ΔN), the electrophilicity index (ω), energy of highest occupied molecular orbital (E_{HOMO}), energy of lowest unoccupied molecular orbital (E_{LUMO}), energy gap (E_{gap}) and Mulliken charge distribution in vacuum and DMSO solvent. Table 7 summarizes the results.

$IP = -HOMO$

$EA = -LUMO$

$\chi = (IP + EA)/2$

$\eta = (IP - EA)/2$

$S = 1/\eta$

$\omega = \chi^2/2\eta$

The energy value of FMSPhDHT's for highest occupied molecular orbital (HOMO) and lowest unoccupied molecular orbital (LUMO) in DMSO

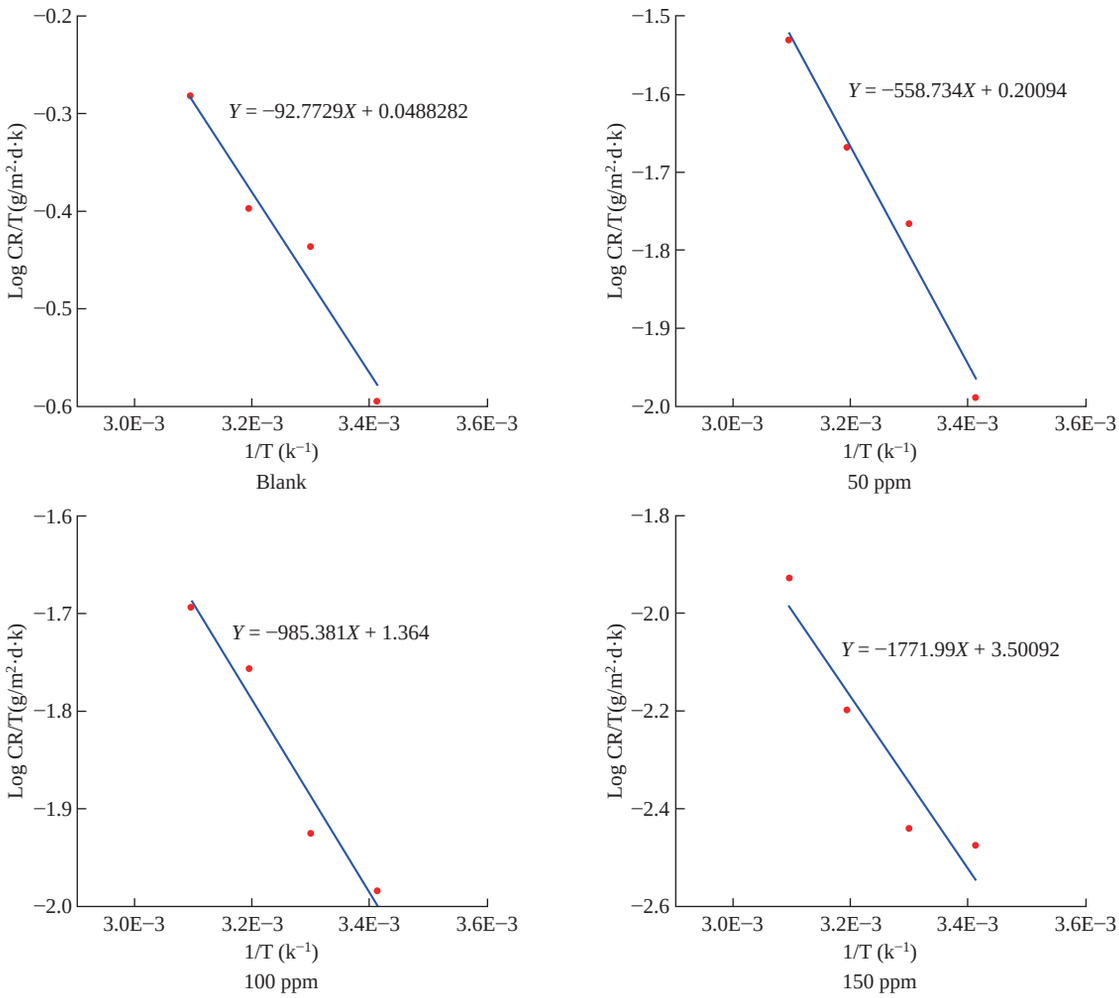

Fig. 6 Transition state plots for carbon steel corrosion in the absence and presence of FMSPHDHT inhibitor.

Table 5 The length of the bond for FMSPhDHT compound using ChemDraw of Mopac tool

Atoms	Bond length (Å)	Atoms	Bond length (Å)
C_{20}-H_{33}	1.095	C_{17}- C_{18}	1.398
C_1-H_{32}	1.1026	C_{16}-C_{17}	1.3908
C_{18}-H_{31}	1.1017	C_{15}-C_{16}	1.4201
C_{17}-H_{30}	1.1026	N_9-C_{15}	1.4455
C_{16}-H_{29}	1.0981	C_{13}-S_{14}	1.5766
N_{12}-H_{28}	1.0074	C_{13}-N_9	1.3386
C_8-H_{27}	1.115	N_{12}-C_{13}	1.3695
C_8-H_{26}	1.1147	N_{11}-N_{12}	1.3483
C_6-H_{25}	1.115	C_{10}-N_{11}	1.2804
C_6-H_{24}	1.1147	N_9-C_{10}	1.4636
C_5-H_{23}	1.0961	S_7-C_8	1.8233
C_4-H_{22}	1.096	C_6-S_7	1.8178
C_1-H_{21}	1.0942	C_3.C_6	1.5048
C_8-C_{10}	1.5105	C_5-C_1)	1.3605
C_{20}-C_{15}	1.4168	C_4-C_5	1.4307
C_{19}-C_{20}	1.3919	C_3-C_4	1.3669
C_{18}-C_{19}	1.3973	O_2 -C_3	1.3685
		C_1-O_2	1.3625

solvent and vacuum are shown in Table 7. One interesting finding is energy value of HOMO for DMSO solvent is great than value in the vacuum. The energy value of HOMO indicates a molecule's ability to donate electrons to an acceptor molecule; in general, the higher the E_{HOMO} value, the greater the molecule's tendency to donate electrons to an acceptor molecule, and the lower the E_{LUMO} value (the molecule's ability to accept electrons), the greater the tendency to accept electrons, As a result of the FMSPhDHT compound's ability to take electrons from metal iron, it has a greater inhibitory efficiency, which is consistent with experimental results [32].

Another important electrical characteristic that emerges from the non-uniform distribution of charges on the various atoms in a molecule is the dipole moment. Stronger intermolecular attraction is caused by higher dipole moments [33]. In the DMSO solvent, the dipole moment of FMSPhDHT is greater than in the vacuum. Adsorption between a chemical substance and a metal surface is likely to be enhanced by a

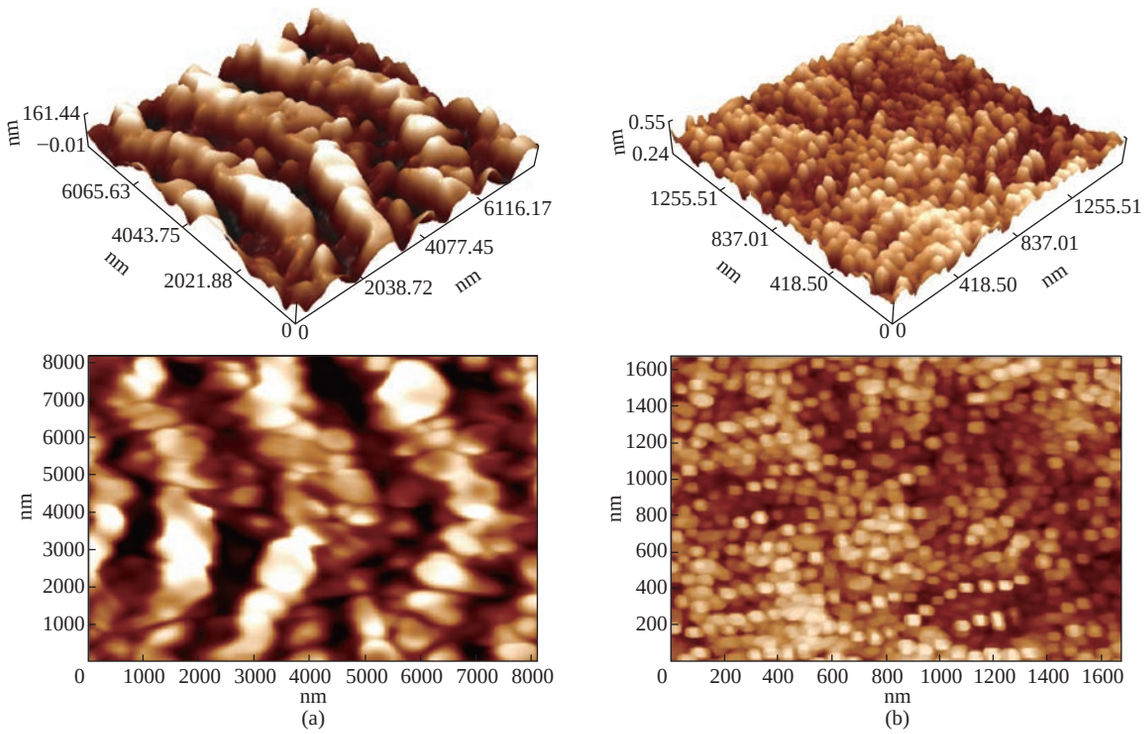

Fig. 7 Micrograph (AFM) of the surface of carbon steel in acidic solution (a) in the absence of an inhibitor (b) in the presence of an inhibitor.

Table 6 Angles of dihedral for FMSPhDHT compound using ChemDraw of Mopac tool

Atoms	Angle of dihedral (deg.)	Atoms	Angle of dihedral (deg.)
S_7-C_8-C_{10}-N_9	-168.802	H_{25}-C_6-S_7-C_8	-60.3329
S_7-C_8-C_{10}-N_{11}	14.1491	O_2-C_3-C_6-S_7	166.7385
H_{26}-C_8-C_{10}-N_9	68.7814	O_2-C_3-C_6-H_{24}	-70.6522
H_{26}-C_8-C_{10}-N_{11}	-108.268	O_2-C_3-C_6-H_{25}	44.9162
H_{27}-C_8-C_{10}-N_9	-49.8947	C_4-C_3-C_6-S_7	-14.2536
H_{27}-C_8-C_{10}-N_{11}	133.0564	C_4-C_3-C_6-H_{24}	108.3558
C_{19}-C_{20}-C_{15}-N_9	-179.915	C_4-C_3-C_6-H_{25}	-136.076
C_{19}-C_{20}-C_{15}-C_{16}	-3.5831	C_4-C_5-C_1-O_2	-0.1084
H_{33}-C_{20}-C_{15}-N_9	0.5644	C_4-C_5-C_1-H_{21}	179.707
H_{33}-C_{20}-C_{15}-C_{16}	176.8964	H_{23}-C_5-C_1-O_2	-179.861
C_{18}-C_{19} - C_{20}-C_{15}	1.0929	H_{23}-C_5-C_1-H_{21}	-0.0453
C_{18}-C_{19}-C_{20}-H_{33}	-179.36	C_3-C_4-C_5-C_1	0.1886
H_{32}-C_{19}-C_{20}-C_{15}	-179.382	C_3-C_4-C_5-H_{23}	179.9414
H_{32}-C_{19}-C_{20}-H_{33}	0.1653	H_{22}-C_4-C_5-C_1	-179.466
C_{17}-C_{18}-C_{19}-C_{20}	1.3599	H_{22}-C_4-C_5-H_{23}	0.2872
C_{17}-C_{18}-C_{19}-H_{32}	-178.169	O_2-C_3-C_4-C_5	-0.2032
H_{31}-C_{18}-C_{19}-C_{20}	179.4038	O_2-C_3-C_4-H_{22}	179.4397
H_{31}-C_{18}-C_{19}-H_{32}	-0.1247	C_6-C_3-C_4-C_5	-179.311
C_{16}-C_{17}-C_{18}-C_{19}	-1.0843	C_6-C_3-C_4-H_{22}	0.3319
C_{16}-C_{17}-C_{18}-H_{31}	-179.13	C_1-O_2-C_3-C_4	0.1383
H_{30}-C_{17}-C_{18}-C_{19}	177.1191	C_1-O_2-C_3-C_6	179.3113
H_{30}-C_{17}-C_{18}-H_{31}	-0.9266	C_5-C_1-O_2-C_3	-0.0136
C_{15}-C_{16}-C_{17}-C_{18}	-1.6563	H_{21}-C_1-O_2-C_3	-179.858
C_{15}-C_{16}-C_{17}-H_{30}	-179.85		
H_{29}-C_{16}-C_{17}-C_{18}	175.7057		
H_{29}-C_{16}-C_{17}-H_{30}	-2.4876		
N_9-C_{15}-C_{16}-C_{17}	-179.774		
N_9-C_{15}-C_{16}-H_{29}	3.0241		
H_{24}-C_6-S_7-C_8	58.2905		

Table 7 Chemical parameters at the quantum level for FMSPhDHT compound calculated using DFT/B3LYP/6-311++G (d, p) in DMSO solvent and vacuum

Parameters	DMSO	Vacuum
Total Energy	-1577.4184 a.u.	-1577.3967 a.u.
HOMO (eV)	-0.2295	-0.21309
LUMO (eV)	-0.04044	-0.04499
E_{gap} (eV)	0.189	0.168
m (Debye)	8.4513	5.7725
IP (eV)	0.2295	0.21309
EA (eV)	0.0404	0.0450
χ (eV)	0.2699	0.2581
h (eV)	0.189	0.1681
S $(eV)^{-1}$	5.291	5.948
w (eV)	0.192	0.198

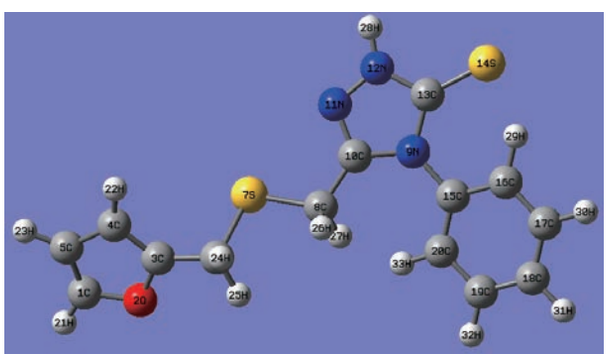

Fig. 8 Optimized geometry of 5-(furan-2-ylmethylsulfonyl-4-phenyl-2,4-dihydro [1,2,4] triazole-3-thione.

strong dipole moment [34]. The inhibitor FMSPhDHT has 8.4513 Debye, this indicates a higher increase in reactivity than the medium without a solvent.

In DMSO solvent and vacuum, the inhibitor's FMSPhDHT electron density distributions, frontier molecular orbital molecular optimization, maximum occupied molecular orbital energy, and lowest unoccupied molecular orbital energy are shown in Fig. 9.

The electronic density of the HOMO molecular orbitals is completely concentrated on the heteroatoms

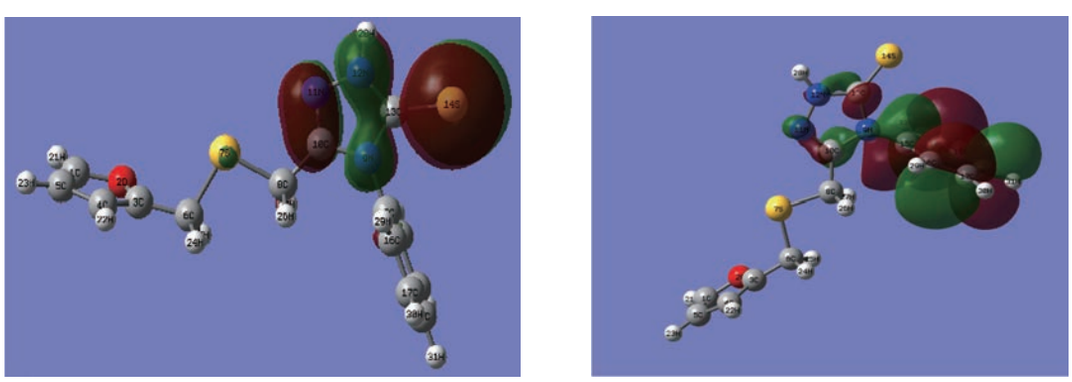

HOMO LUMO

(I)

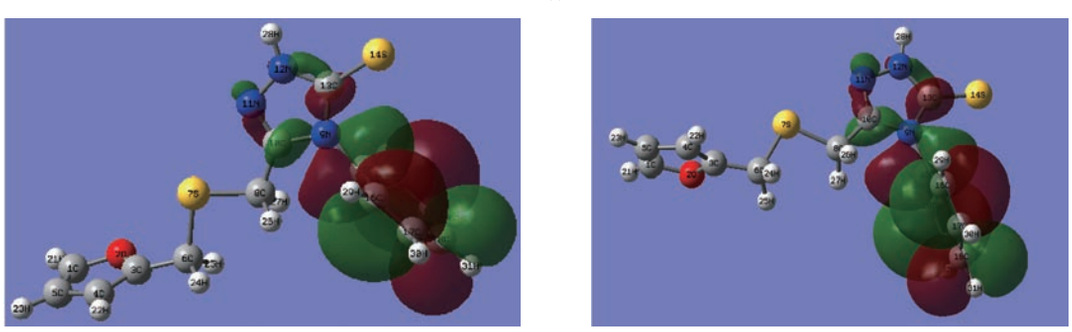

DMSO Vacuum

(II)

Fig. 9 (I) HOMO and **(II)** LUMO in DMSO solvent and vacuum of the inhibitor FMSPhDHT using DFT/B3LYP/6-311 ++G (d, p).

three nitrogen atoms and sulfur, but the LUMO molecular orbitals exhibit an important electronic density scattered throughout the majority of the phenyl ring and a small density over 3 nitrogen atoms (triazole ring). This finding is consistent with the Mulliken charge distribution and the direction of the dipole moment seen in Fig. 10 and stated in Table 8.

Active sites of the inhibitor

Mulliken charges distribution (MCD) are an important characteristic to consider when investigating the adsorption center of inhibitor compounds. FMSPhDHT molecule has greater nucleophilic and electrophilic electrical charge values in DMSO than in vacuum [35]. Mulliken's charge population study for the FMSPhDHT molecule in two mediums (DMSO and vacuum) and the direction of dipole moment are shown in Fig. 10 and Table 7.

In order to investigate the effects of charge distribution on the adsorption process. Table 8 shows the order of the nucleophilic reactive sites of

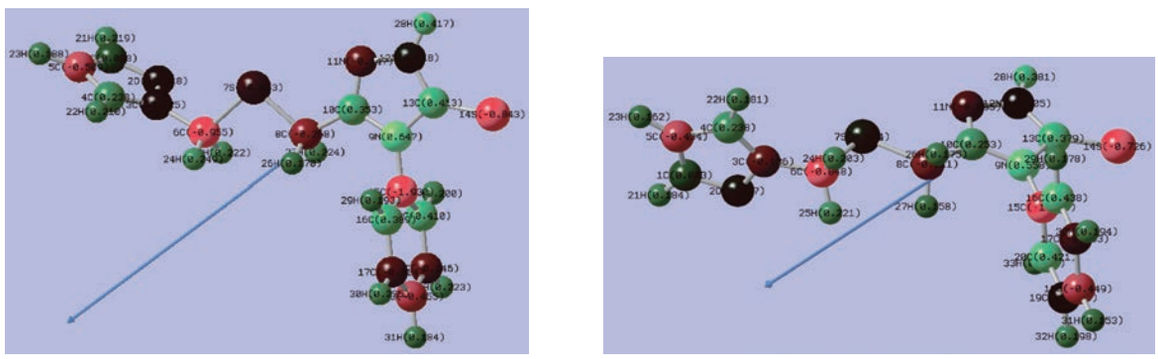

DMSO Vacuum

Fig. 10 Atomic charge distributions for the FMSPhDHT compound.

Table 8 Mulliken charge values of the FMSPhDHT compound

Symbol of Atom	C1	O2	C3	C4	C5
MCD	0.083* 0.083**	0.017 -0.018	-0.136 -0.025	0.238 0.238	-0.454 -0.5092
Symbol of Atom	C6	S7	C8	N9	C10
MCD	-0.848 -0.954	0.024 -0.063	-0.211 -0.268	0.558 0.647	0.253 0.353
Symbol of Atom	N11	N12	C13	S14	C15
MCD	0.095 -0.147	-0.005 0.017	0.379 0.413	-0.726 -0.843	-1.948 -1.930
symbol of Atom	C16	C17	C18	C19	C20
MCD	0.438 0.389	-0.083 -0.113	-0.449 -0.455	-0.008 -0.146	0.421 0.410
Symbol of Atom	H21	H22	H23	H24	H25
MCD	0.18 0.218	0.181 0.210	0.162 0.187	0.203 0.248	0.221 0.221
Symbol of Atom	H26	H27	H28	H29	H30
MCD	0.175 0.169	0.158 0.224	0.381 0.417	0.178 0.193	0.194 0.224
Symbol of Atom	H31	H32	H33		
MCD	0.153 0.183	0.198 0.223	0.163 0.200		

* vacuum, ** DMSO

FMSPhDHT inhibitor is as follows: $C_{15} > C_6 > S_{14} > C_5 > C_{18} > C_8 > N_{11} > C_{19}$, while the order of the electrophilic reactive sites is as follows $N_9 > C_{13} > S_{20} > C_{16} > C_{10}$. The most interesting aspect of this results, is that FMSPhDHT molecule is an effective inhibitor that matches experimental results [36-37].

As well as to charge distribution study, the electrostatic potential (ESP) map is a common tool for detecting where a molecule's electron density is high or low. Electrostatic potential may be used to forecast the reaction center of molecules when they come into contact with other materials. Figure 11 shows the electrostatic potential (ESP) map derived using the B3LYP/6-31++G(d,p) approach. The locations with the highest positive, negative, and zero electrostatic potential, respectively, are represented by the blue, red, and green regions in Fig. 11. According to Fig. 11, the largest negative electron density zone is found near S_{14}, N_9, C_{13}, C_{15}, S_7, N_{11}, C_6 whereas the positive electron density region is mostly found in hydrogen and certain carbon atoms as well as phenyl ring.

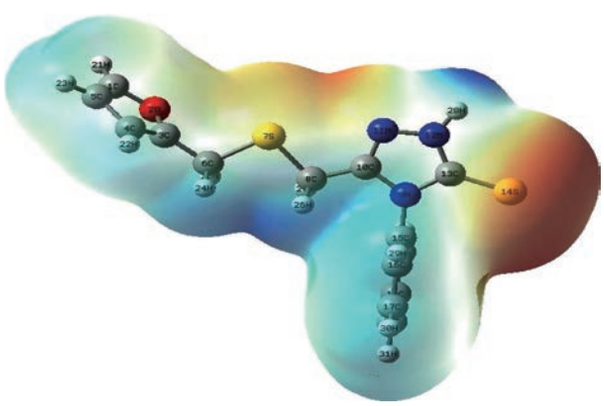

Fig. 11 Electrostatic potential (ESP) maps for the studied FMSPhDHT compound.

The electrostatic potential results were in accord with the charge distribution results when it came to the influence of hetero atoms on the adsorption of the FMSPhDHT compound on the surface of carbon steel and its resistance to corrosion in an acidic medium [38].

Conclusion

The following are some of the study's findings:

- The experimental results revealed that the novel furan derivative 5-(furan-2-ylmethylsulfonyl-4-phenyl-2,4-dihydro [1,2,4] triazole-3-thione (FMSPhDHT) is an efficient corrosion inhibitor for carbon steel in acidic solutions.

- The investigated inhibitor's corrosion inhibition efficacy was 99.4 percent.

- The inhibitor reduced the thermodynamic feasibility of corrosion by increasing ΔG^* values, which were positive and rose marginally as temperature climbed. While the system›s entropy decreases as a result of the thermodynamic analysis.

- The creation of a protective barrier on the carbon steel surface is suggested by the potentiodynamic polarization curve and AFM investigation.

- DFT (B3LYP/6-311 ++G(d,p) based quantum chemistry calculations of parameters related to the electronic structures of FMSPhDHT back up the experimental findings.

- The charge distribution research revealed the impacts of FMSPhDHT on the adsorption process by revealing nucleophilic and electrophilic inhibitor reactive sites.

The findings show that the FMSPhDHT compound is a potential inhibitor that may be utilized to reduce the corrosion of oil tanker pipes as well as prevent corrosion of metal mechanisms in industrial facilities.

Conflict of Interests

The authors declare that no competing interest exists.

References

[1] Cherrak, K., Dafali, A., Elyoussfi, A., et al. Two new benzothiazine derivatives as corrosion inhibitors for mild steel in hydrochloric acid medium. *J. Mater. Environ. Sci.*, 2017, 8(2), 636-647.

[2] Ouici, H., Tourabi, M., Benali, O., Selles, C., Jama, C., Zarrouk, A., Bentiss, F. Adsorption and corrosion inhibition properties of 5-amino 1,3,4-thiadiazole-2-thiol on the mild steel in hydrochloric acid medium: thermodynamic, surface and electrochemical studies. *J. Electroanal. Chem.*, 2017, 803: 125-134.

[3] Ansari, K.R., Quraishi, M.A., Singh, A. Schiffs base of pyridyl substituted triazoles as new and effectivecorrosion inhibitors for mild steel in hydrochloric acid solution. *Corros. Sci*., 2014, 79: 5-15.

[4] Benali, O., Larabi, L., Traisnel, M., Gengembre, L., Harek, Y. Electrochemical, theoretical and XPS studies of 2-mercapto-1-methylimidazole adsorption on carbon steel in 1 M $HClO_4$. *Appl. Surf. Sci*., 2007, 253(14): 6130-6139.

[5] Cano, E., Polo, J.L., Iglesia, A.La., Bastidas, J.M., 2004. A study on the adsorption of benzotriazole on copper in hydrochloric acid using the inflection point of the isotherm. *Adsorption*, 10(3), 219-225.

[6] Lebrini, M., Traisnel, M., Lagrene'e, M., Mernari, B., Bentiss, F. Inhibitive properties, adsorption and a theoretical study of 3,5-bis(n-pyridyl)-4-amino-1,2,4-

triazoles as corrosion inhibitors for mild steel in perchloric acid. *Corros. Sci.*, 2008, 50(2): 473-479.

[7] Kubba R.M., Mohammed M.A. and Ahamed L.S. DFT Calculations and Experimental Study to Inhibit Carbon Steel Corrosion in Saline Solution by Quinoline-2-One Derivative: Carbon Steel Corrosion. *Baghdad Science Journal*. 2021, 18(1): 0113.

[8] Kubba R.M. and Mohammed M.A. Theoretical and Experimental Study of Corrosion Behavior of Carbon Steel Surface in 3.5% NaCl and 0.5 M HCl with Different Concentrations of Quinolin-2-One Derivative. *Baghdad Sci. J*., 2022, 19(1): 0105.

[9] Loto R.T., Loto C.A., Joseph O. and Olanrewaju G. Adsorption and corrosion inhibition properties of thiocarbanilide on the electrochemical behavior of high carbon steel in dilute acid solutions. *Results in Physics*, 2016, 6: 305-314.

[10] Kacimi Y. El, Azaroual M.A., Touir R., Galai M. and Alaoui K. Corrosion inhibition studies for mild steel in 5.0 M HCl by substituted phenyltetrazole, Euro-Mediterr. *J Environ Integr*, 2017, 2: 1-11.

[11] Haque J., Verma C., Srivastava V., Quraishia M.A. and Ebenso Eno E. Experimental and quantum chemical studies of functionalized tetrahydropyridines as corrosion inhibitors for mild steel in 1 M hydrochloric acid. *Results in Physics*, 2018, 9: 1481-1493.

[12] Kannan P., Shukla S.K., Rao T.S. and Rajendran N. Adsorption, thermodynamic and quantum chemical studies of 3-(4-Chlorobenzoylmethyl) benzimidazoliumbromide in inhibition effect on carbon steel, *J. Mater. Environ. Sci*., 2016, 7(4): 1154-1171,

[13] Luma S.A. Synthesis of New Five-Membered Hetrocyclic Compounds from 2-Furfuryl Mercaptan Derivative and Evaluation of their Biological Activity, *J. Glob. Pharma. Technol.*, 2018, 11: 298.

[14] AL-Sammarraie A.M. Role of carbon dioxide on the corrosion of carbon steel reinforcing bar in simulating concrete electrolyte. *Baghdad Science Journal*, 2020, 17(1): 93.

[15] Sherine B., Nasser A.J.A. and Rajendran S. Inhibitive action of hydroquinone- Zn_2-system in controlling the corrosion of carbon steel in well water. *Inter. J. Eng., Sci., Tech.*, 2010, 2(4): 341-357.

[16] Khudhair N.A., Synthesis, identification and experimental studies for carbon steel corrosion in hydrochloric acid solution for polyimide derivatives. AIP Conference Proceedings. Vol. 2290. No. 1. AIP Publishing LLC, 2020.

[17] Khudhair N.A., Khadom M.M. and Khadom A.A. Effect of Trimethoprim Drug Dose on Corrosion Behavior of Stainless Steel in Simulated Human Body Environment: Experimental and Theoretical Investigations. *Journal of Bio-and Tribo-Corrosion*, 2021, 7(3): 1-15.

[18] Benali, O., Larabi, L., Tabti, B., Harek, Y. Influence of 1-methyl 2-mercapto imidazole on corrosion inhibition of carbon steel in 0.5 M H_2SO_4. Anti-Corros. Method Mater. 2005, 52: 280-285.

[19] Fusco M.A., Yasar Ay, Casey A.H.M., Bourham M.A. and Winfrey A.L. Corrosion of single layer thin film protective coatings on steel substrates for high level waste containers, *Journal Progress in Nuclear Energy*, 2016, 89: 159-169.

[20] El Ouali I., Hammouti B., Aouniti A., Ramli Y., Azougagh M. and Essassi E.M. Thermodynamic characterisation of steel corrosion in HCl in the presence of 2-phenylthieno (3,2-b) quinoxaline. *Journal of Materials and Environmental Science*, 2010, 1(1): 1-8.

[21] Kubba R.M. and Al-Joborry N.M. Theoretical and Experimental Study of a New Imidazo (1,2-a) Pyridine Derivative as a Corrosion Inhibitor for the Carbon Steel Surface in the Saline Media. *ANJS*, 2020, 23(1): 13-26.

[22] Oguzie E.E. Corrosion inhibition of aluminium in acidic and alkaline media by Sansevieria trifasciata extract. *Corrosion Science*, 2007, 49(3): 1527-1539.

[23] Ahamad I. and Quraishi M.A. Bis (benzimidazol-2-yl) disulphide: an efficient water soluble inhibitor for corrosion of mild steel in acid media, *Corros. Sci.*, 2009, 51: 2006-2013.

[24] Al-Mashhdani H.A.Y., Al-Saadie K.A., Hayfaa A.A. and Duha A. Cactus as a green inhibitor for the corrosion of carbon steel in seawater, *PCAIJ*, 2015, 10(4): 111-120,

[25] A Rehan T., Lami N.A., and Khudhair N.A. Synthesis, characterization and anti-corrosion activity of new triazole, thiadiazole and thiazole derivatives containing imidazo [1,2-a] pyrimidine moiety. *Chemical Methodologies*, 2021: 285-295.

[26] AL-Thib A.T. and Khudhair N.A. Spectroscopic study of some aromatic hydrazones derivated from aromatic substituted benzophenones and benzaldydes. *PCAIJ*, 2016, 11(1): 24-33.

[27] Zaafarany I. Phenyl phthalimide as corrosion inhibitor for corrosion of C-Steel in sulphuric acid solution. *Portugaliae Electrochimica Acta*, 2009, 27(50): 631-643.

[28] Lee C., Yang W. and Parr G.G. Development of the Colle-Salvetti correlation-energy formula into a functional of the electron density. *Phys. Rev.*, 1988, B37(2): 785-789.

[29] Frisch M.J., Trucks G.W., Schlegel H.B., Scuseria G.E., Robb M.A., Cheeseman J.R., Scalmani G., Barone V., Mennucci B., Petersson G.A., Nakatsuji H., Caricato M., Li X., Hratchian H.P., Izmaylov A.F., Bloino J., Zheng G., Sonnenberg J.L., Hada M., Ehara M., Toyota K., Fukuda R., Hasegawa J., Ishida M., Nakajima T., Honda Y., Kitao O., Nakai H., Vreven T., Montgomery Jr J.A., Peralta J.E., Ogliaro F., Bearpark M., Heyd J.J., Brothers E., Kudin K.N., Staroverov V.N., Kobayashi R., Normand J., Raghavachari K., Rendell A., Burant J.C., Iyengar S.S., Tomasi J., Cossi M., Rega N., Millam J.M., Klene M., Knox J.E., Cross J.B., Bakken V., Adamo C., Jaramillo J., Gomperts R., Stratmann R.E., Yazyev O., Austin A.J., Cammi R., Pomelli C., Ochterski J.W., Martin R.L., Morokuma K., Zakrzewski V.G., Voth G.A., Salvador P., Dannenberg J.J., Dapprich S., Daniels A.D., Farkas Ö., Foresman J.B., Ortiz J.V., Cioslowski J. and Fox D.J. Gaussian 09; Gaussian, Inc, *Journal Wallingford, CT*, 2009, 32: 5648-5652.

[30] Rauk A. Orbital interaction Theory of Organic Chemistry. 2001, 2nd Ed, John Wiley & Sons: NewYork.

[31] Singh A., Ansari K.R., Kumar A., Liu W., Songsong C. and Lin Y. Electrochemical, surface and quantum chemical studies of novel imidazole derivatives as corrosion inhibitors for J55 steel in sweet corrosive environment. *J. Alloys Compd.*, 2017, 712: 121-133.

[32] Jisha M., Zeinul Hukuman N.H., Leena P. and Abdussalam A.K. Electrochemical, computational and adsorption studies of leaf and floral extracts of Pogostemon quadrifolius (Benth.) as corrosion inhibitor for mild steel in hydrochloric acid, *J. Mater. Environ. Sci.*, 2019, 10(9): 840-853.

[33] Dwivedi A. and Misra N. Quantum chemical study of Etodolac (Lodine), Der Pharma Chemica.2010, 2(2): 58-65.

[34] Li X., Deng S., Fu H. and Li T. Adsorption and inhibition effect of 6- benzylaminopurine on cold rolled steel in 1.0 M HCl, Electrochim. *Acta*, 2009, 54: 4089-4098.

[35] Ramya K. and Joseph A. Synergistic effects and hydrogen bonded interaction of alkyl benzimadazoles and thiourea pair on mild steel in hydrochloric acid, *J. Taiwan Inst. Chem. Eng.*, 2015, 52: 127-139.

[36] Fergachia O., Benhibae F., Rbaab M., Touira, D.R. and

Ouakkic M. Experimental and Theoretical Study of Corrosion Inhibition of Mild Steel in 1.0 M HCl Medium by 2(-4(hloro phenyl-1H-benzo[d]imidazol)-1-yl)phenyl) methanone, *Mater. Res.*, 2018, 21: 1-11.

[37] Tian U. and Yuan K. Performance and Mechanism of Alkylimidazolium Ionic Liquids as Corrosion Inhibitors for Copper in Sulfuric Acid Solution. *Molecules*, 2021, 26(16): 4910.

[38] Tian U. and Yuan K. Performance and Mechanism of Alkylimidazolium Ionic Liquids as Corrosion Inhibitors for Copper in Sulfuric Acid Solution. *Molecules*, 2021, 26(16): 4910.